Systematic and Applied Microbiology 42 (2019) 135–144

Contents lists available at ScienceDirect

Systematic and Applied Microbiology

journal homepage: http://www.elsevier.com/locate/syapm

Autofluorescent characteristics of *Candidatus* Brocadia fulgida and the consequences for FISH and microscopic detection

Jörg Böllmann*, Steffen Engelbrecht, Marion Martienssen

Department of Biotechnology for Water Treatment, BTU-Cottbus-Senftenberg, Siemens-Halske-Ring 8, 03046 Cottbus, Germany

ARTICLE INFO

Article history:
Received 19 June 2018
Received in revised form 10 August 2018
Accepted 13 September 2018

Keywords:
16S rDNA
Hydrazine synthase *hzsA*
Hydrazine oxidase *hzo*
FISH
Candidatus Kuenenia stuttgartiensis
Candidatus Brocadia fulgida

ABSTRACT

An enrichment culture of *Candidatus* Brocadia fulgida was identified by three independent methods: analysis of autofluorescence using different microscope filter blocks and a fluorescence spectrometer, fluorescence *in situ* hybridization (FISH) with anammox-specific probes and partial sequencing of the 16S rDNA, hydrazine synthase *hzsA* and hydrazine oxidoreductase *hzo*. The filter block BV-2A (400–440, 470 LP, Nikon) was suitable for preliminary detection of *Ca.* B. fulgida. An excitation-emission matrix revealed three pairs of excitation-emission maxima: 288–330 nm, 288–478 nm and 417–478 nm. Several autofluorescent cell clusters could not be stained with DAPI or by FISH, suggesting empty but intact cells (ghost cells) or inhibited permeability. Successful staining of autofluorescent cells with the FISH probes Ban162 and Bfu613, even at higher formamide concentrations, suggested insufficient specificity of Ban162. Under certain conditions, *Ca.* B. fulgida lost its autofluorescence, which reduced the reliability of autofluorescence for identification and detection. Non-fluorescent *Ca.* Brocadia cells could not be stained with Ban162, but with Bfu613 at higher formamide concentrations, suggesting a dependency between both parameters. The phylogenetic analysis showed only good taxonomical clustering of the 16S rDNA and *hzsA*. In conclusion, careful consideration of autofluorescent characteristics is recommended when analysing and presenting FISH observations of Ca. B. fulgida to avoid misinterpretations and misidentifications.

Introduction

Anammox (anaerobic ammonium oxidizing) bacteria have been reported from many ecosystems and manmade habitats [3,18]. Their anaerobic chemolithoautotrophic equimolar conversion of ammonia and nitrite into nitrogen gas plays an important role in the global nitrogen cycle besides denitrification [23] and might ameliorate the negative effects of excess anthropogenic nitrogen [15,24]. In several ecosystems, this has been suggested as the main nitrogen sink [37]. The anammox process is a promising tool for removing nitrogen, especially from nitrogen-rich and carbon-poor wastewaters [49], although handling is difficult and the growth rate is very slow [23]. Nevertheless, besides many small-scale approaches, the process has been implemented successfully several times in large-scale wastewater treatment plants [49].

The five known *Candidatus* genera Kuenenia, Scalindua, Brocadia, Jettenia and Anammoxoglobus are monophyletic and deeply branched from within the *Planctomycetes* [7,37,45]. Culture-independent methods, such as fluorescence *in situ* hybridization (FISH), the amplification and sequencing of the 16S rDNA or other anammox-specific genomic regions, such as hydrazine oxidase (*hzo*) or hydrazine synthase (*hzs*) targeted by many anammox-specific primer sets [33,32,17], are the most common tools for detection and identification of these bacteria [10]. Hydrazine synthase produces hydrazine, a unique anammox intermediate from nitric oxide and ammonium, and it has been used as a specific biomarker for anammox bacteria [16,17,25]. Hydrazine oxidoreductase is an essential enzyme that dehydrogenates hydrazine to dinitrogen gas [25], and it was the first functional gene used for detecting anammox bacteria [16]. It has been found in many different types of environments [16,32] and, although many sequences are available, only a few identified sequences have been published [7,9,17,20,26,33,52]. Therefore, genomic data banks still require reliably identified sequences in order to provide sufficient information for the identification of the rapidly increasing number of shot gun sequences and for detailed phylogenetic analysis. Moreover, identification by sequencing is often limited by few database entries of identified strains that have poor coverage [15,52].

For FISH, there are many available probes for different taxonomic specificities [45], making this method a powerful tool for

* Corresponding author.
E-mail address: boellman@b-tu.de (J. Böllmann).

https://doi.org/10.1016/j.syapm.2018.09.002
0723-2020/

the identification of anammox species. However, failures of this technique have also been reported [21,34].

In addition to molecular techniques, a so far unique autofluorescence characteristic of *Candidatus* Brocadia fulgida was identified several years ago by Kartal et al. [27] and the study is still the only detailed analysis of this tendency. These authors reported two excitation maxima at 352 and 442 nm with corresponding emission maxima at 464 and 521 nm. The appearance was described as doughnut-shaped in contrast to the commonly reported crested- or sickle-shaped form of anammox cells after FISH or DAPI staining [29]. Although many studies have referred to this characteristic, autofluorescence has only been reported a few times [12,13,26,45], and has barely been acknowledged in the literature [8]. On the contrary, it might have been unintentionally combined with FISH analysis eventually causing misinterpretation [19].

The current study presents the identification of a *Ca.* B. fulgida [26] enrichment biomass, the second candidatus status in the Brocadia cluster besides *Ca.* B. anammoxidans, *Ca.* B. sinica [23] and *Ca.* B. caroliniensis [50]. *Ca.* B. fulgida can outcompete other anammox species by utilizing acetate as an electron source [22,23,27] and could be successfully combined with denitrifying bacteria at elevated carbon concentrations [21]. It is been used in full-scale anammox wastewater treatment plants [17] in combination with the nitrifying and denitrifying bacteria [31] found in granules in a single stage sequencing batch reactor [34] or as biofilm in moving bed reactors [51]. It is also present in aquatic, especially fresh water, environments [20,53]. The species was identified by staining with taxon-specific FISH (fluorescence *in situ* hybridisation) probes and sequencing of 16S rDNA, hydrazine synthase (*hzsA)* and hydrazine oxidoreductase (*hzo*) gene fragments that also included a phylogenetic analysis. Detailed measurements of the autofluorescent pattern were also provided, which were slightly different to previous reports [27], and its consequences for FISH analysis and its suitability for detection and identification are discussed. We also question the taxonomic specificity of the FISH probe Ban162 and autofluorescence as a truly unique feature of *Ca.* B. fulgida. The results are compared with a second enrichment culture containing *Ca.* B. fulgida and *Ca.* K. stuttgartiensis in order to verify the findings. As a result, autofluorescence in combination with an appropriate filter set is suggested as a suitable method for detecting and identifying *Ca.* B. fulgida under specific conditions. However, we also report the disappearance of the autofluorescence and discuss the possible causes.

Materials and methods

Origin of the biomass

In this study, the autofluorescent characteristics of two different anammox enrichment cultures were compared. The first was provided by another institution, originally classified as *Candidatus* B. anammoxidans, and was further cultivated and enriched in a laboratory-scale bioreactor consisting of a 1 L Schott glass bottle with an airtight four-port cap. Over a period of 1.5 years, the content of the reactor was discontinuously mixed by a magnetic stirrer at 300 rpm for 15 min every 30 min. During this time, a major proportion of the biomass became loosely attached to the inner walls of the glass bottle. The reactor was kept in the dark at a room temperature between 16 and 20 °C with a pH between 7.8 and 8.4. The reactor was fed *via* a peristaltic pump with 50–100 mL day^{-1} synthetic medium [11] containing between 1 to 5 g L^{-1} $(NH_4)_2SO_4$ and 0.8 to 4 g L^{-1} KNO_2 or occasionally with ammonia and nitrite enriched effluent from a nearby wastewater treatment plant (mean BOD_5: 5 mg L^{-1}, mean pH: 7.0). Ammonia was added at a ratio of 1.1–1.4 (NH_4-N):1(NO_2-N), which was above the suggested ratio of 1:1.3 [47] to avoid ammonia limitation and enable potential nitrification to eliminate uncontrolled minimal oxygen input *via* the apparatus tubes and joints. The feed concentrations of ammonia and nitrite were adjusted according to the consumption to maintain the nitrite reactor concentration below 1 mM in order to avoid an uncontrolled increase above inhibiting concentrations [49]. The feed was always flushed with nitrogen gas for 30 min and 1 min with CO_2 to balance the pH between 6.8 and 7.5. For performance tests, synthetic medium with a retention time of 2.4 days was used. During the performance tests, the feed concentration was increased stepwise. The reactor could metabolize up to 98 mg NH_4-N and 135 mg NO_2-N per litre and day at a ratio (NH_4-N:NO_2-N) of 1:1.38 ± 0.18 (n = 18). The enrichment of the anammox biomass could only be estimated as approximately 50% by FISH and by autofluorescence observations (as described below), since the anammox clusters were very difficult to break apart.

The second biomass was taken from another laboratory-scale reactor containing a mixture of *Ca.* B. fulgida and *Ca.* K. stuttgartiensis (60% and 40% of the total anammox biomass) [6]. The bacteria grew as a biofilm and the reactor was run under high saline conditions for more than 6 months prior to analysis with $NaNO_2$ and NH_4Cl as nitrogen sources.

Sample preparation, DNA extraction and PCR

DNA from 200 μL fresh biomass was extracted with extraction buffer/chloroform and isopropanol according to Rathsack et al. [41]. The DNA samples were resuspended in 100 μL nuclease free water (Quiagene). The PCR mix contained pure water (13.4 μL), DreamTaq™ GreenBuffer (Thermo Fisher Scientific) + $MgCl_2$ (2.5 μL), forward and reverse primers (TIB Molbiol, Germany) (1 μL, 25 μM), BSA (1 μL, 20 mg mL^{-1}), dNTP (0.5 μL, 10 mM), DMSO (0.5 μL), DreamTaq™ DNA Polymerase (Thermo Fisher Scientific) (0.1 μL, 5U) and 5 μL DNA extract from a stepwise ten-fold dilution series to exclude possible contamination and inhibitors. Three different regions of the genome were amplified and sequenced. The 16S rDNA was amplified with the anammox-specific forward primers Pla46F (GAC TTG CAT GCC TAA TCC) [36] and Amx368 (TTC GCA ATG CCC GAA AGG) [22], and the reverse primer brod1260r (GGA TTC GCT TCA CCT CTC GG) [39], the universal primer 1392r (ACG GGC GGT GTG TAC) [39] and Amx820 (AAA ACC CCT CTA CTT AGT GCCC) [5], which is more specific to the *Ca.* Kuenenia-Brocadia cluster [44]. The genomic DNA of the hydrazine synthase *hzsA* subunit was amplified and sequenced with the forward primers hzsA_526F (TAY TTT GAA GGD GAC TGG) [17] and hzsA_1597F (WTYGGKTATCARTATGTAG) [17] and the reverse primer hzsA_1857R (AAABGGYGAATCATARTGGC) [17]. A third region of the genomic DNA of hydrazine oxidase was sequenced with the primer pair hzo AB4 F (TTG ART GTG CAT GGT CTA WTG AAAG) and hzo AB4 R (GCT GAC CTG ACC ART CAGG) [18]. DNA was amplified with a thermal cycler Primus 96 plus (MWG-Biotech AG) and the following protocols: 16S rDNA for 5 min at 94 °C, 10 cycles for 60 s at 94 °C, 60 s at 50 °C, 90 s at 72 °C and 20 cycles for 60 s at 94 °C, 60 s at 54 °C, 60 s at 72 °C and final annealing for 10 min at 72 °C; *hzsA* and *hzo* fragments for 5 min at 94 °C, 30 cycles for 60 s at 94 °C, 60 s at 54 °C, 90 s at 72 °C and final elongation 10 min at 72 °C. PCR products were visualized with a one-fold TAE buffered agarose gel (1% for 16S rDNA, 1.5% for *hzsA* DNA, 100 V, 60 min), stained with ethidium bromide (0.2 mg L^{-1}) and compared to a MassRuler DNA Ladder Mix (Thermo Scientific, Schwerte, Germany). For sequencing, the PCR products of the highest dilution step with a solid band were used. The PCR products were sequenced with BigDye Version 1.1 and the sequencer Abi Prism 310 at the Carl-Thiem-Hospital, Cottbus. Sequences were edited and aligned with BioEdit 7.2.5 [14] and compared against the NCBI GenBank database using a BLAST

Table 1
Name, excitation and emission wavelengths of fluorescence microscope long-pass filter sets used to determine the autofluorescent properties of *Candidatus* Brocadia species.

Filter set	Excitation	Emission
UV-2A	330–380	420 LP
BV-2A	400–440	470 LP
B-2A	450–490	515 LP
G-2A	510–560	590 LP

search. The sequences obtained were deposited in the database under accession numbers KU682542 and KY780955.1 (16S rDNA), KU682543, KX227384 and MH366514 (*hzsA*), and KU682543.1 and KY780956.1 (*hzo*). Phylogenetic trees were constructed with the software MEGA 6.06 [48] by combining own sequences with the most related sequences from a BLAST search and representative identified examples of the other anammox genera obtained from NCBI. The maximum likelihood, neighbor-joining and minimum-evolution methods were compared in combination with bootstrap reliability tests (500 cycles).

Autofluorescence analyses

Autofluorescence and FISH analyses were performed with an epifluorescence microscope (Nikon Eclipse LV 100 with a DS-Fi1 camera), the filters listed in Table 1 and the Nikon software NIS-Elements BR. All filter sets were the long-pass filter type, which lets light above a specific wavelength pass through. For detailed measurements, photomicrographs of the same region of interest (ROI, 10 × 10 μm) were taken with all available filter sets (Table 1). The colour photomicrographs were split into the three RGB channels (Fig. 2) and the mean pixel intensity (range 0–255) of the ROI for each channel was measured and the sum of the intensities was calculated (Fig. 3).

The autofluorescence was further analysed using a microplate Labsystems Fluoroskan II (GMI Inc.) reader. Samples from the reactor were ultrasonically treated (Sonorex Super RK 510H, BANDELIN electronic GmbH & Co., KG, Germany) for 4 min. Then, 200 μL were placed into six wells that were measured three times at all available and possible combinations of excitation (355, 485, 544 and 584 nm) and emission wavelengths (460, 538, 590 and 612 nm). To combine the results of both experiments, the emission intensity was normalised to a percentage scale with blue emission at a UV-excitation representing 100%.

Finally, the autofluorescence of both anammox enrichment cultures was analysed with an Aqualog fluorescence spectrometer (Aqualog 3.6.7.43, HORIBA Scientific, HORIBA Jobin Yvon GmbH, Germany) by creating a three dimensional excitation-emission matrix (EEM; for example see Ref. [2]). The biomass was homogenized by sonication to disperse larger flocks and clusters to avoid rapid sedimentation. Subsamples were centrifuged for 10 min at 5000 *g* and the autofluorescent properties of the cell-free supernatant were analysed. The feeds for both cultures were also analysed to exclude the components of the media as a source of autofluorescence. The data were processed with the software Origin Pro 8.5.1. (OriginLab Corporation, USA). In addition, the emission intensity was measured at different optical densities to determine the influence of turbidity on the fluorescence measurements.

Fluorescence in situ *hybridization*

FISH samples were prepared according to established protocols (Table 2) [3,26,43] from appropriate diluted samples fixed with 4% paraformaldehyde solution, washed with phosphate buffered saline (PBS), air dried on a hybridization slide and dehydrated with ethanol. Samples were hybridized with the Texas Red-labelled probes Pla46 specific for *Planctomycetales*, and therefore for all anammox bacteria [3,36], Ban162 specific for *Ca.* B. anammoxidans [45], Bfu613 specific for *Ca.* B. fulgida [27], and Kst157 specific for *Ca.* K. stuttgartiensis [43]. Samples were analysed with the G-2A filter block (Table 1) on a Nikon Eclipse LV 100. As a positive control for successful hybridization, subsamples were hybridized with EUB338-I [3]. As a counterstain and to support the detection of DNA in the cells, some samples were counter stained with DAPI (1 $\mu g\,mL^{-1}$). The sensitivity of the probes Ban162 and Bfu613 were later increased by increasing the formamide concentration twice from 40% to 45% and 50%, and from 30% to 35% and 40%, respectively, with the corresponding salt concentrations in the washing buffer (Table 2).

Results and discussion

Autofluorescence

The autofluorescence of the reactor biomass was microscopically studied with excitation wavelengths from UV light to green light, and emission in the range from blue to red. Except for the red emission, there was always significant autofluorescence visible (Figs. 1 and 5). The excitation range of 400–440 nm (filter set BV-2A) resulted in the highest emission intensities in all RGB cannels (Figs. 1 and 2a). It was twofold, fourfold and tenfold compared to UV, blue and green excitation, respectively. The sum of the intensities, the combined mean intensity within the ROI of all three RGB (red, green, blue) channels (Fig. 2b), was highest (600) at an excitation wavelength of 400–440 nm (filter set BV-2A) compared to 200 at ultra-violet excitation (UV-2A: 330–380 nm), 50 at blue excitation (B-2A: 450–490 nm), and only 2.5 at green excitation (G-2A).

With the microplate reader, autofluorescence was highest at the available excitation wavelength 355 nm (UV). It was 100% (20.6) at blue emission (emission filter 460 nm), only 25% (5.2) at 538 nm (green), and 6% (1.3) at 590 nm (Fig. 2a). Excitation at 485 nm resulted in an emission of 26% (5.4), whereas the emissions at the remaining combinations were below 10% compared to the best combination (Table 2).

The results suggested an autofluorescence maximum at an excitation wavelength between UV light (330–380 nm) and blue light (450–490 nm) in the range of the BV-2A filter set (400–440) with an emission maximum between blue and green.

Subsequent detailed measurement with a fluorescence spectrometer revealed three pairs of excitation and emission maxima at 288:330 nm (270–295 nm:315–360 nm), 288:478 nm (270–295 nm:460–510 nm) and 414:478 nm (380–430 nm:450–520 nm) (Figs. 3 a and 4). All pairs were caused by the biomass and seemed to belong to particulate matter or were strongly associated with the biomass, since the centrifuged reactor medium and reactor feed were non-fluorescent (Supplementary Fig. A). The first pair was far below the performance of regular microscopes and natural visibility. The pair at 261–478 nm seemed to be negligible compared to the pair at 288–478 nm. The emission intensity at 478 nm after 417 nm excitation was approximately 80% of the emission at 330 nm after 288 nm excitation. The emission intensity at 478 nm after 288 nm excitation was approximately 35% compared to the emission at 330 nm. In addition to the measured emission maxima, contrary dependencies of the emission intensity to increasing optical densities of the sonicated biomass were observed at different wavelengths (Fig. 3b). At 288 nm excitation, the emission intensity at 330 nm increased steadily with increasing amounts of suspended solids. The emission intensity at 478 nm after 288 nm emission remained roughly constant but with a decreasing tendency. The intensity of

Table 2
Formamide concentration in the hybridization buffer and corresponding salt concentration in the washing buffer for the different FISH probes applied.

Probe	Formamide %	NaCl mM	Sequence
EUB338-I [3]	0–50	0–0.2	5′-GCTGCCTCCCGTAGGAGT-3′
Pla46 [3,36],	30	0.1	5′-GACTTGCATGCCTAATCC-3′
Kst157 [43]	25	0.15	5′-GTTCCGATTGCTCGA AAC-3′
Bfu613 [27]	30	0.1	5′-GGATGCCGTTCTTCCGTTAAGCGG-3′
Ban162 [45]	40	0.046	5′-CGGTAGCCCCAATTGCTT-3′
Bfu613	35	0.07	
Ban162	45	0	
Ban162 + Bfu613	40	0.046	
Ban162	50	0	

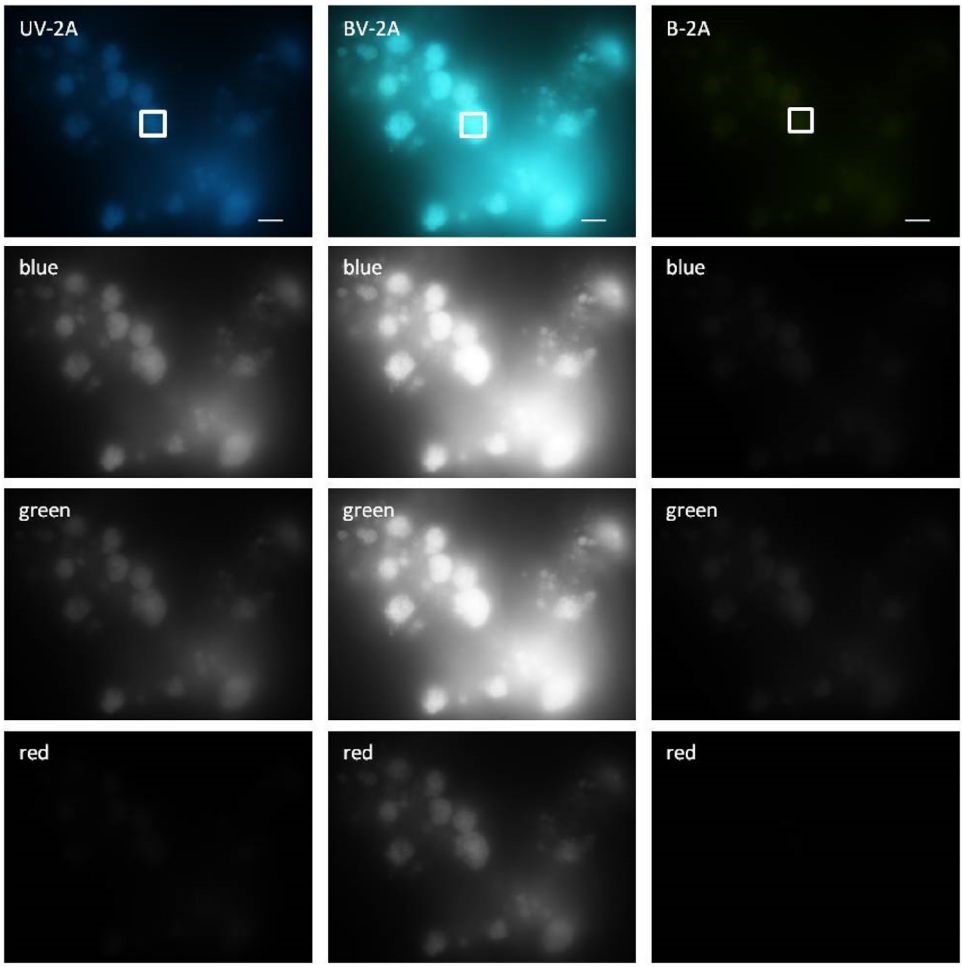

Fig. 1. Fluorescence microscope photomicrographs of autofluorescent anammox biomass (excitation at 330–380, 400–440 and 450–490 nm) as combined RGB channels (top) and separate RGB channels (grey scale) for a better comparison of the emission intensity. The square marks the area of emission intensity measurement (region of interest: ROI). Bar = 10 μm.

the most important and unique autofluorescence (417–478 nm) reached the highest values at the tested OD of 0.15 with a strong decline at higher suspended solid concentrations. Therefore, it is recommended that similar tests are performed with different ODs when analysing autofluorescence by photometric methods.

Detailed analyses of the second biomass revealed a fluorescence maximum at 330 nm after 288 nm excitation, which was clearly visible in the cell suspension and the cell free supernatant (Fig. 3c and d). Autofluorescence was produced by the biomass, since the feed was not fluorescent. However, compared to the first described *Ca.* B. fulgida biomass it was not strongly associated with the cells, since it was caused by suspended or dissolved substances as well. The other peaks of the pure *Ca.* Brocadia biomass (288–478 nm and 417–478 nm) were missing in the mixed enrichment culture. Apparently *Ca.* B. fulgida lost its autofluorescent properties at 288–478 nm and 417–478 nm under the conditions in the second enrichment culture, which was confirmed microscopically by non-fluorescent but Bfu613-stained cell clusters (Supplementary Fig. B). Several reasons for the loss of autofluorescence are possible: different osmolarity caused by higher salt concentrations in the second mixed culture, the use of $NaNO_2$ and NH_4CL instead of KNO_2 and $(NH_4)_2SO_4$, or an unknown type of interaction or competition between both anammox species.

The observed autofluorescence of *Ca.* B. fulgida has already been described by Kartal et al. [26,27] and by Schmid et al. [45] for an incompletely described species. However, they observed only two excitation maxima at 352 and 442 nm with corresponding emission maxima at 464 and 521 nm, which was quite different to the

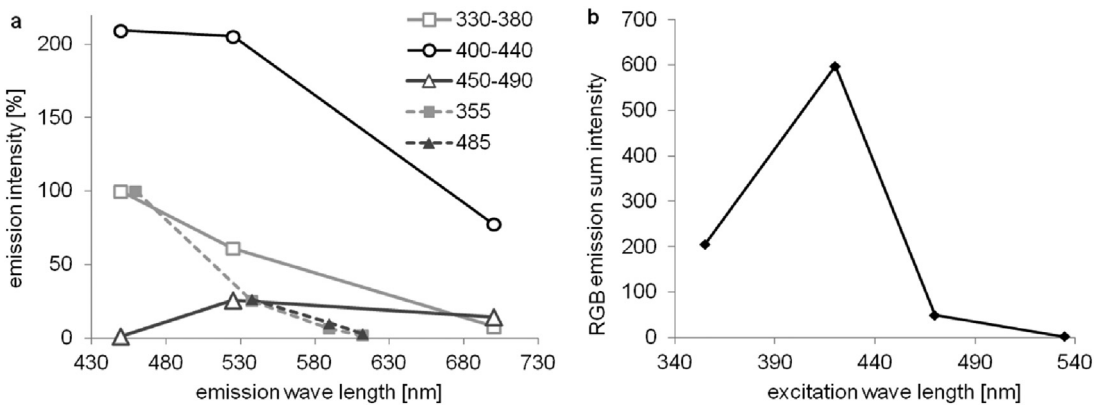

Fig. 2. a: Emission intensity of autofluorescent anammox biomass at different excitation wavelengths (caption) measured as individual RGB channels using a fluorescence microscope (solid lines) and by a microplate reader (dotted lines). Emission at UV excitation = 100%; **b:** mean sum emission intensity of all RGB channels of the pixel within the ROI measured with a fluorescence microscope.

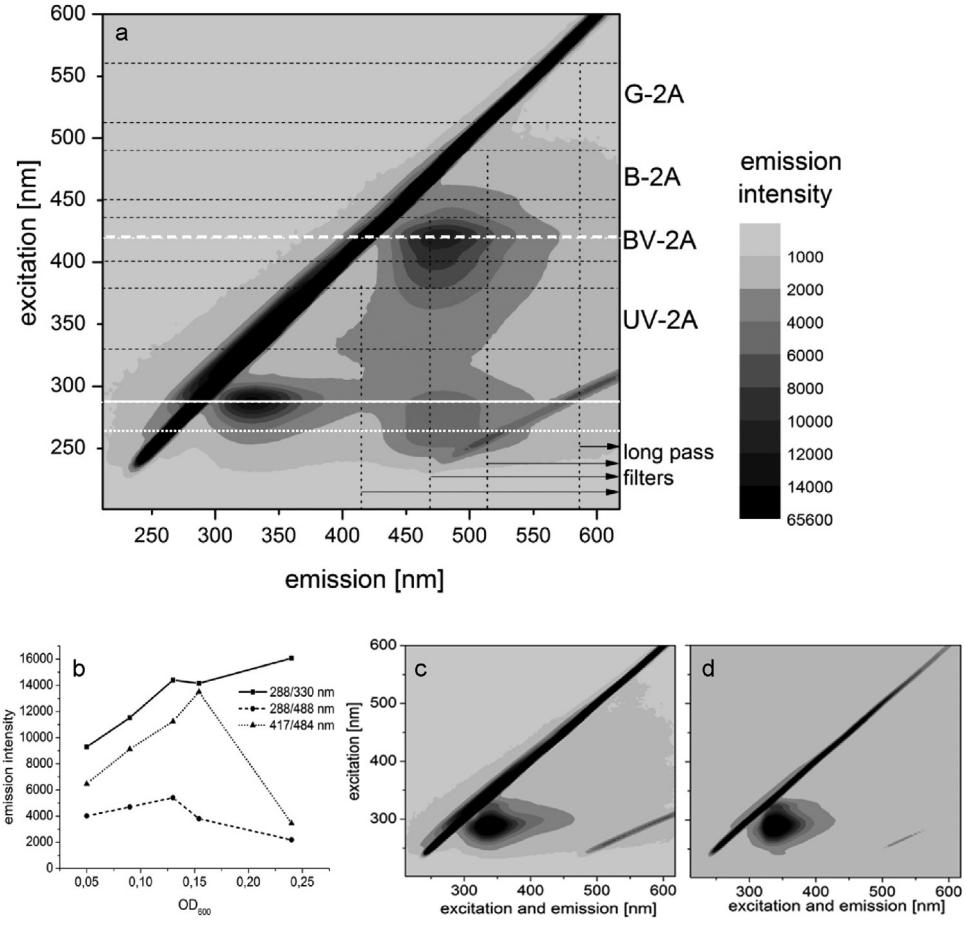

Fig. 3. a: Autofluorescent properties of *Candidatus* Brocadia fulgida at excitation wavelengths from 210 to 600 nm and emission wavelengths from 211 to 620 nm. Darker areas indicate increasing emission intensities. Horizontal dotted lines indicate the excitation wavelength of different microscope filters, whereas vertical dotted lines together with the arrows indicate the emission wavelength of the long-pass filters. The horizontal white lines show the transects of the emission curves in Fig. 4 with the corresponding line shape. The diagonal dark area is the result of light dispersion caused by the turbidity of the biomass solution (Rayleigh-Tyndall effect); **b**: dependency of the emission intensity at different wavelengths and different optical densities (OD_{600}); **c** and **d**: autofluorescent properties of a second anammox enrichment biomass containing *Ca.* K. stuttgartiensis and *Ca.* B. fulgida, as well as the supernatant of centrifuged biomass. The emission intensity is in arbitrary intensity units.

observations in the current study. Kartal et al. [27] suggested that EPS polymers were responsible for the *Ca.* Brocadia autofluorescence, while Van de Graaf et al. [11] reported strong absorption at 420 nm caused by increasing cytochrome content for an incompletely described anammox species, which might correspond to our observed excitation maximum at 417 nm. The BV-2A filter has been used previously by Kastner et al. [28] for the detection and quantification of methanogenic *Archaea*. For these bacteria, different factors or coenzymes, especially F_{350} and F_{420}, have accounted for this type of autofluorescence [4,28,46]. With regard to the spectrophotometric results and the microscopic observations, it was assumed that the 478 nm autofluorescent substances or structures were certainly

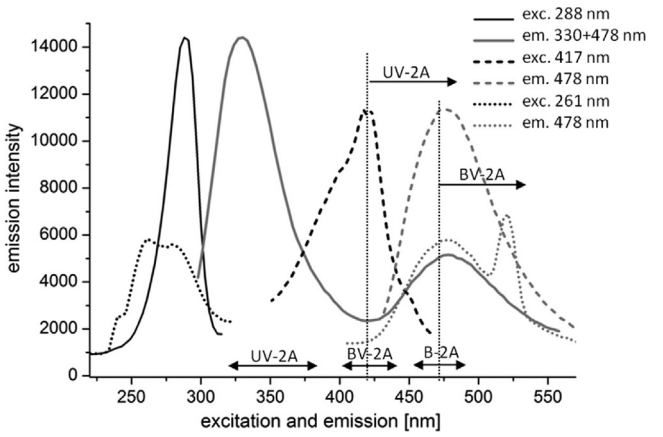

Fig. 4. Excitation and emission maxima at different corresponding wavelengths (black: excitation, grey: emission) for a suspension of *Ca.* B. fulgida (OD_{600} 0.13): excitation maxima at 288 nm (solid), 417 nm (dashed) and 261 nm (dotted); emission maxima at 330 nm (solid), 478 nm (solid, dashed and dotted). The peak at 550 nm is an instrumental artefact, double arrows indicate the wavelength of the excitation filters, and simple arrows indicate the long-pass emission filter. The y-axis is in arbitrary intensity units.

outside the cell but strongly associated with the cells. A previously proposed autofluorescent EPS could be a likely explanation for this phenomenon. However, the identification of the substances and a possible correlation with environmental conditions, activity or stress needs further research. Nevertheless, it is not certain at this point whether these characteristics are unique to *Ca.* B. fulgida or are shared by other *Ca.* Brocadia species due to the poor coverage in the literature. The origin of the autofluorescence at 330 nm remains unclear, since several substances are fluorescent in this region [2].

Under the microscope, larger clusters especially showed fluorescence, although smaller groups and single cells did as well (Figs. 2 and 5). Only the margin of the cells was fluorescent, the cell interior remained dark. The autofluorescent structures could be described as hollow- or doughnut-shaped (Fig. 5), which has been described previously by Kartal et al. [26,27]. The photomicrographs of an incompletely identified *Ca.* Brocadia strain by Güven et al. [12,13] suggested a similar morphology. The stained structures after application of FISH and DAPI, however, were rather sickle-shaped, as described for anammox bacteria in general [30] due to the large anammoxosome [29,26], and they were clearly inside the autofluorescent ring (Fig. 5). In contrast to Kartal et al. [27], autofluorescent single cells could be detected in untreated fresh samples, although this might be the result of sample preparation or stirring in the reactor. Photomicrographs from another study [8] have suggested similar observations.

It was further concluded that the detection of autofluorescence at 410–425 nm excitation and 460–480 nm emission wavelengths (filter set BV-2A) in combination with the unique morphology of the fluorescent structures could be used as a first and simple method for detection and identification of *Ca.* B. fulgida directly in native and conserved samples. However, the absence of this fluorescence cannot exclude the presence of *Ca.* B. fulgida, since autofluorescence is not present under certain conditions, as shown in this study. Consequently, additional molecular tests will be essential in order to confirm the detection. Furthermore, only the combination with FISH or DAPI can truly detect living *Ca.* B. fulgida cells, since the fluorescent structures remained intact even after assumed cell death.

Fluorescence in situ *hybridization*

The strong autofluorescence of the first described *Ca.* B. fulgida biomass in blue and green might have had a large influence on the FISH analyses. In the study, green autofluorescence was as bright as the red FISH signal, which might be misinterpreted as positively green-labelled bacteria (Fig. 6). This type of interference by autofluorescence with FISH measurements has already been mentioned by Kartal et al. [27]. Therefore, it was concluded that some reported observations of FISH-labelled *Ca.* Brocadia cultures [12,13] might have been affected by this autofluorescence, either causing misinterpretation [19] or eventually leading to false positive or at least altered FISH signals. Therefore, great care must be taken when single or mixed cultures of *Ca.* B. fulgida are analysed microscopically, and comparison with non-labelled biomass is recommended when fluorescence microscope observations of *Ca.* Brocadia biomass are being reported.

Texas Red-labelled FISH probes were used because of the strong green autofluorescence. The probes Pla46, Ban162 and Bfu613 successfully labelled the autofluorescent biomass at commonly applied formamide concentrations (Figs. 5–7, Supplementary Fig. B), whereas Kst157 did not stain any cells. In the first described pure *Ca.* Brocadia enrichment culture, all FISH positively stained cells were autofluorescent. However, not all autofluorescent cell clusters could be stained with either DAPI or FISH probes, as seen in Fig. 7 and Supplementary Fig. C in the red circles, suggesting empty dead cells (ghost cells) with an intact autofluorescent cell wall or EPS. EPS impermeability was also possible but in our opinion this was less likely, since no differences were observed in the autofluorescent intensity and morphology between stained and non-stained cells. According to Schmid et al. [45], probe Ban162 is specific for *Ca.* B. anammoxidans, while Bfu613 is specific for *Ca.* B. fulgida [27]. Nevertheless, the same autofluorescent biomass could be stained with both probes (Supplementary Fig. B) at published stringencies. Assuming a mixed culture, similar autofluorescent patterns of both species could explain this observation, although autofluorescence has been described to date only for *Ca.* B. fulgida. In addition, the sequencing results suggested only the presence of *Ca.* B. fulgida. On the other hand, if autofluorescence was truly unique to *Ca.* B. fulgida, Ban162 was less specific than assumed and labelled *Ca.* B. fulgida as well, which has not been reported to date in the literature. A BLAST (NCBI) search revealed 100% identity of Bfu613 with our and other *Ca.* B. fulgida isolates, such as JQ864319.1. Surprisingly, a 100% match was also found with *Ca.* Kuenenia entry KX020506.1, although this might have been a misidentification. For Ban162, several 100% matches were found with *Ca.* B. caroliniensis KF810110.1, JF487828.1, *Ca.* B. fulgida DQ459989.1, EU478693.1 and *Ca.* B. anammoxidans, AF375994.1. These findings supported the assumption that Ban162 was not as specific as originally reported. However, since the probe was designed more than a decade ago based on a much smaller number of sequences the specificity could not be estimated any better at that time.

The specificity of both probes (Ban162 and Bfu613) was further tested on both anammox enrichment cultures with stepwise increasing formamide concentrations in comparison to the commonly used 30% and 40% (probeBase [1,8,27,32,40]), which should have increased the sensitivity of the probes. Bfu631 and EUB338-1 could stain both enrichment cultures also at 35% and 40% formamide concentrations (Supplementary Fig. B). Ban162 could stain the autofluorescent biomass at 45% and 50% (Supplementary Fig. B), whereas it failed at a concentration of 45% for the second mixed non-fluorescent culture (Supplementary Fig. B). Since there was always high variability in the fluorescence intensity between different cell clusters, a change of fluorescence intensity between different formamide concentrations could not be confirmed. Most of the Ban162 negative cells were stained with DAPI (Supplementary Fig. B), which excluded the possibility of empty dead cells. Therefore, it is proposed that Ban162 is not specific for *Ca.* B. anammoxidans at the established formamide concentration of 40%, but

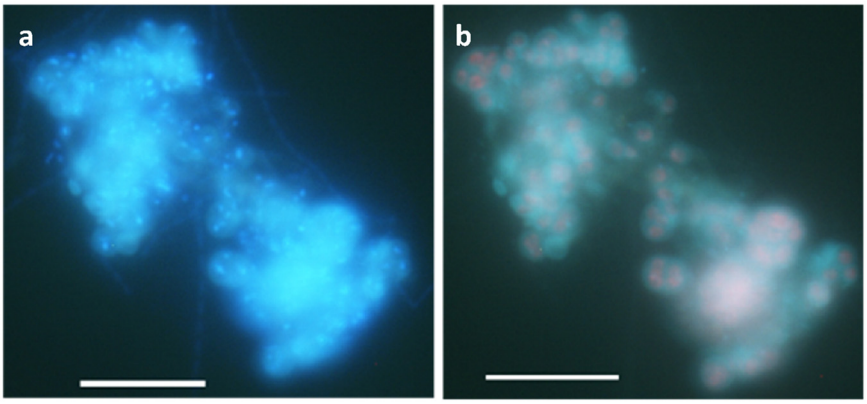

Fig. 5. a: Combination of autofluorescence and DAPI staining; **b:** combination of autofluorescence and FISH (Bfu631). Bar = 10 μm.

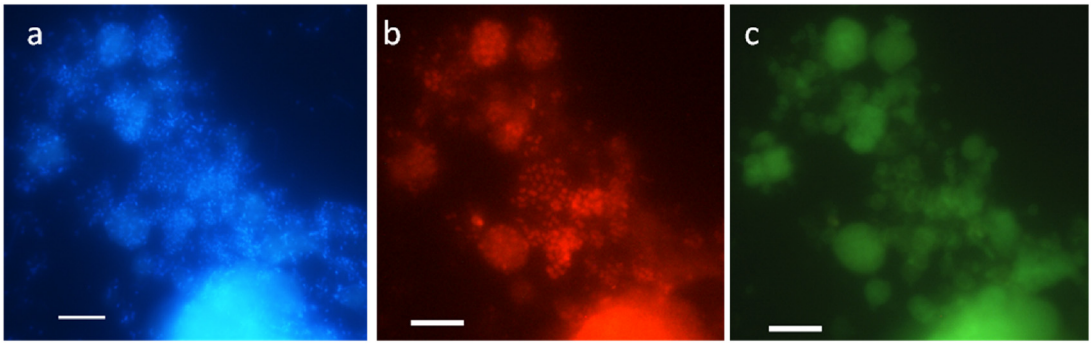

Fig. 6. Fluorescence microscope photomicrographs of anammox biomass stained with DAPI (a), FISH probe Pla46 (b), and showing autofluorescence with filter set B-2A (c). Bar = 10 μm.

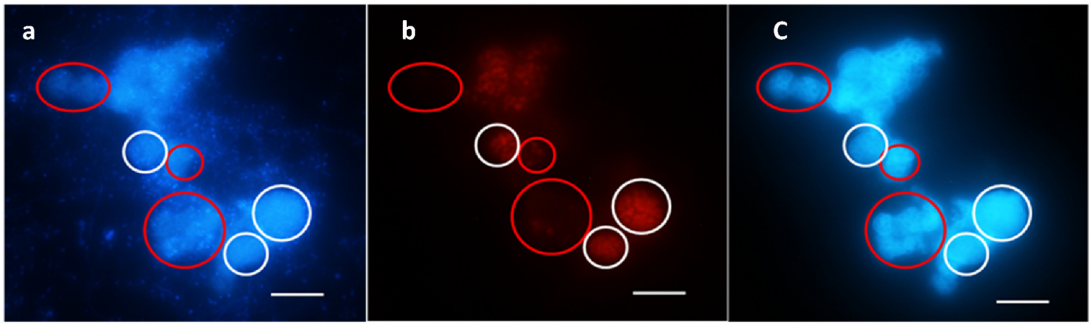

Fig. 7. Fluorescence microscope photomicrographs of anammox biomass stained with DAPI (a), FISH probe Pla46 (b), and showing autofluorescence (c). Red circles indicate areas with DAPI and an autofluorescent signal but with no signal after FISH staining, whereas white circles indicate areas with signals after all three treatments. Bar = 10 μm. (For interpretation of the references to color in this figure legend, the reader is referred to the web version of this article.)

it can stain *Ca.* B. fulgida under certain conditions even at 50% formamide. Since Ban162 binds within the helical structure of 16S rRNA, an optimum concentration of formamide is especially important in order to open the helix, although this is also difficult to predict. Eventually, other older FISH probes need to be re-evaluated for their optimum stringency and specificity regarding the much larger number of available sequences. Apparently, the autofluorescent property has an influence on FISH staining, either during binding or the removal of the FISH probes, although the reasons for this phenomenon remain unclear. Whether this has caused misidentification in previous studies cannot be concluded but it seems possible, since the *Ca.* Brocadia biomass described here was originally identified as *Ca.* B. anammoxidans BY Ban162 and it was autofluorescent from the beginning. In this context, the co-occurrence of both species tested by FISH [8] might be questionable.

PCR and sequencing

The identification by fluorescence microscopy and FISH was confirmed by the sequencing of three different regions: 16S rDNA, *hzsA* and *hzo*. The comparison of the obtained 16S rDNA sequence with other entries listed in the NCBI GenBank resulted in only a few matches with identified entries having 95% identity or more, including *Ca.* B. fulgida [52], *Ca.* B. sinica [38], *Ca.* B. caroliniensis [50] and *Ca.* B. anammoxidans [42]. The *Ca.* Brocadia culture in the current study fitted well in the *Ca.* Brocadia cluster and was nearly identical with other *Ca.* B. fulgida entries (Fig. 8a), which supported the previous identification. All three tree-building procedures used resulted in similar phylogenetic trees with slightly different bootstrap values. Generally, all anammox genera clustered very well, and identification with the 16S region seemed very reliable, which has also been reported by other studies [16,35,40]. However, dur-

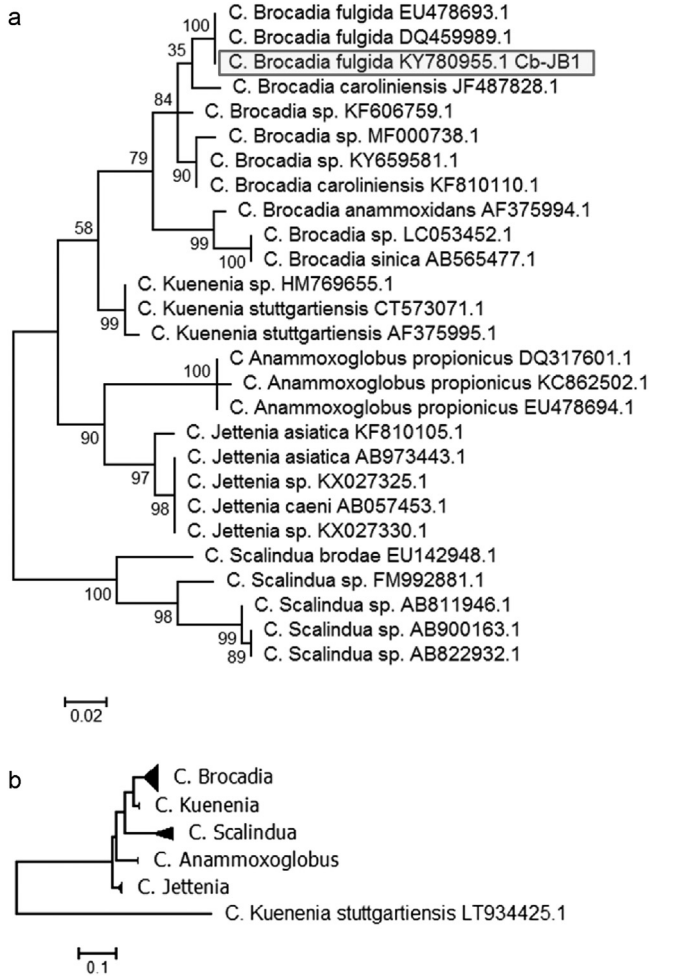

Fig. 8. a: 16S maximum likelihood in combination with the bootstrap reliability tests (500 cycles) with the entry from this study marked; **b:** phylogenetic tree with an additional entry for *Ca.* K. stuttgartiensis. Other genera branches from **a**. are collapsed. The bar indicates 2% and 10% estimated sequence divergence respectively.

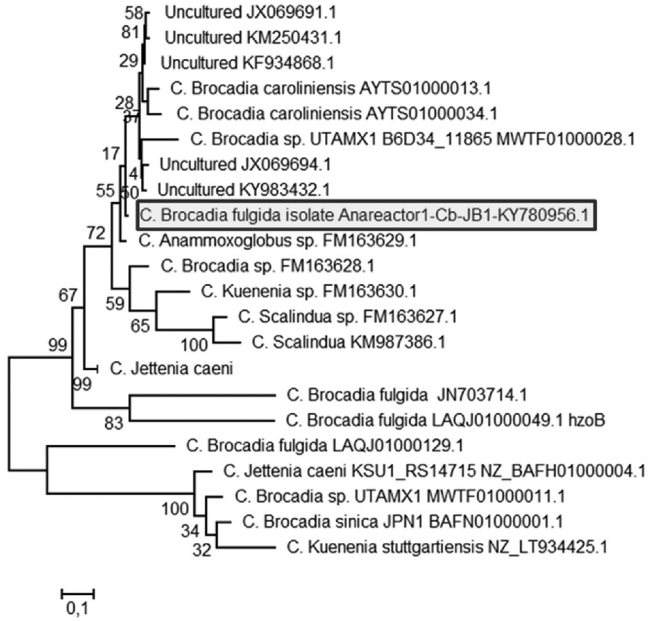

Fig. 9. *hzoAB* maximum likelihood in combination with the bootstrap reliability tests (500 cycles). The entry from this study is marked. The bar indicates 10% estimated sequence divergence respectively.

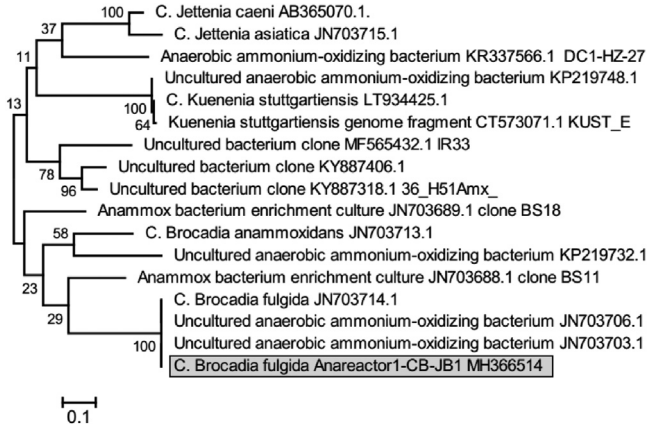

Fig. 10. *hzsA* maximum likelihood in combination with the bootstrap reliability tests (500 cycles). The entry from this study is marked. The bar indicates 10% estimated sequence divergence respectively.

ing the analysis, one *Ca.* K. stuttgartiensis (LT934425.1) entry did not fit this assembly (Fig. 8b) but the reason remained speculative. Several distinct clusters of *Ca.* K. stuttgartiensis have at least been reported based on the *hzo* gene sequence [16,33], although incorrect identification or editing also seems possible.

In contrast to the 16S rDNA entries, the number of identified *hzo* sequences was very low for all anammox genera. As seen in Fig. 9, there was no clustering of the anammox groups, and the sequence was not closely associated with other *Ca.* B. fulgida entries, although it was very similar to many unidentified GenBank entries. Therefore, reliable identification would have been impossible. The results of the amino acid sequence analysis were similar to the nucleotide sequences in that the groups were not well clustered and the entry from the current study was not closely associated with the other *Ca.* B. fulgida records. Consequently, for a detailed phylogenetic analysis, more identified sequences and further studies would be needed.

The sequence of the *hzsA* subunit was related most closely to one entry identified as *Ca.* B. fulgida [17] with 100% identity and 100% coverage, and to other unidentified sequences (Fig. 10). All other matches had less than 60% coverage or 99% or less percentage identity. Among these were entries of *Ca.* B. anammoxidans and *Ca.* J. asiatica with 82% identity. The few identified sequences of *Ca.* Brocadia, *Ca.* Kuenenia and *Ca.* Jettenia clustered well. Overall, the number of identified sequences was very low, which reduced the suitability of the *hzsA* subunit as a reliable tool for identification.

Conclusions

The study successfully identified an anammox enrichment culture as *Candidatus* Brocadia fulgida with three independent techniques. Microscopically observed autofluorescence together with the specific morphology described as doughnut-shaped confirmed previous descriptions. However, by generating an excitation-emission matrix the measured maxima were different to previous descriptions. Therefore, the microscope filter set BV-2A or other filters covering the excitation and emission maxima of 417–478 nm are recommended for fast specific detection of this species, assuming that *Ca.* B. fulgida is the only species with this characteristic. However, the absence of autofluorescence does not guarantee the absence of this species, since the documented loss of autofluorescence under certain, as yet unspecified, conditions can result in false negative results. Confirmation by FISH or molec-

ular tools is therefore necessary. In the first enrichment culture, only autofluorescent cells could be stained equally by FISH with probes Ban162 and Bfu613, even at 10% higher stringencies, and all stained cells were autofluorescent. Either *Ca.* B. anammoxidans is also autofluorescent, which has not been reported previously, or the Ban162 probe is not as specific under certain conditions as previously assumed, which is supported by 100% matches with various *Ca.* Brocadia GenBank entries. In the second enrichment culture, the *Ca.* Brocadia-specific stained cells were consistently non-fluorescent and both probes stained equally under standard conditions. However, at slightly increased specificity (5% increased formamide concentration) only Bfu613 could stain the biomass. Therefore, it was assumed that only *Ca.* B. fulgida was present and that Ban162 could not differentiate between both *Ca.* Brocadia species under certain conditions. However, similar tests with a *Ca.* B. anammoxidans biomass are needed to support this argument.

The combination of FISH and DAPI staining with the autofluorescence observation revealed large numbers of morphologically intact fluorescent cells, which could not be stained by both methods and appeared hollow. The autofluorescent structures (cell wall or EPS) of these ghost cells seemed to remain intact even after cell death. Therefore, cell counts based on autofluorescence, optical densities or dry weight would overestimate the quantity of metabolically active biomass. Nevertheless, it could be possible that dead cells of other anammox species also remain intact causing similar measurement problems. In this study, FISH analysis or q-PCR seemed important for verifying the health of the biomass and the number of living cells. The structures or substances responsible for the visible autofluorescence were strongly associated with the cells and were not dissolved in the media, since the autofluorescence disappeared after centrifugation. Although it is good laboratory practice, the importance of comparing FISH-labelled anammox biomass with untreated controls and the use of correct protocols should be emphasised, since the described autofluorescence could disguise or create false FISH signals leading to misinterpretations. Finally, with the sequencing of three different DNA fragments and the good match with published sequences of *Ca.* B. fulgida in combination with the other applied methods, it was possible to confirm the identification and previous descriptions of the species, as well as providing new identified sequences needed for further phylogenetic studies.

Acknowledgements

This study was carried out in conjunction with the research project Nitrolimit (www.nitrolimit.de; Fkz. 033L041D) and the Anammox II (AIF KF2950901SA1) project. We would like to thank the associated master and bachelor students Uche Dickson and Lisa Vieweger for their support, and Isaac Mbir Bryant for proof reading. Special thanks also to CTK Cottbus for sequencing and to the Chair of Hydrology at BTU Cottbus-Senftenberg for the opportunity to use the spectrophotometer.

Appendix A. Supplementary data

Supplementary data associated with this article can be found, in the online version, at https://doi.org/10.1016/j.syapm.2018.09.002.

References

[1] Almstrand, R., Persson, F., Daims, H., Ekenberg, M., Christensson, M., Wilén, B.-M., Sörensson, F., Hermansson, M. (2014) Three-dimensional stratification of bacterial biofilm populations in a moving bed biofilm reactor for nitritation-anammox. Int. J. Mol. Sci. 15, 2191–2206, http://dx.doi.org/10.3390/ijms15022191.

[2] Carstea, E.M., Bridgeman, J., Baker, A., Reynolds, D.M. (2016) Fluorescence spectroscopy for wastewater monitoring: a review. Water Res. 95, 205–219, http://dx.doi.org/10.1016/j.watres.2016.03.021.

[3] Dapena-Mora, A., van Hulle, S.W., Luis Campos, J., Méndez, R., Vanrolleghem, P.A., Jetten, M. (2004) Enrichment of anammox biomass from municipal activated sludge: experimental and modelling results of anammox enrichment. J. Chem. Technol. Biotechnol. 79, 1421–1428, http://dx.doi.org/10.1002/jctb.1148.

[4] Doddema, H.J., Vogels, G.D. (1978) Improved identification of methanogenic bacteria by fluorescence microscopy. Appl. Environ. Microbiol. 36, 752–754.

[5] Egli, K., Fanger, U., Alvarez, P.J.J., Siegrist, H., van der Meer, J.R., Zehnder, A.J.B. (2001) Enrichment and characterization of an anammox bacterium from a rotating biological contactor treating ammonium-rich leachate. Arch. Microbiol. 175, 198–207, http://dx.doi.org/10.1007/s002030100255.

[6] Engelbrecht, S., Mozooni, M., Rathsack, K., Böllmann, J., Martienssen, M. (2018) Effect of increasing salinity to adapted and non-adapted anammox biofilms. Environ. Technol., 1–9, http://dx.doi.org/10.1080/09593330.2018.1455748.

[7] Ferousi, C., Speth, D.R., Reimann, J., Op den Camp, H.J., Allen, J.W., Keltjens, J.T., Jetten, M.S. (2013) Identification of the type II cytochrome c maturation pathway in anammox bacteria by comparative genomics. BMC Microbiol. 13, 265, http://dx.doi.org/10.1186/1471-2180-13-265.

[8] Figueroa, M., Vázquez-Padín, J.R., Mosquera-Corral, A., Campos, J.L., Méndez, R. (2012) Is the CANON reactor an alternative for nitrogen removal from pretreated swine slurry? Biochem. Eng. J. 65, 23–29, http://dx.doi.org/10.1016/j.bej.2012.03.008.

[9] Gori, F., Tringe, S.G., Folino, G., van Hijum, S.A., Op den Camp, H.J., Jetten, M.S., Marchiori, E. (2013) Differences in sequencing technologies improve the retrieval of anammox bacterial genome from metagenomes. BMC Genomics 14, 7, http://dx.doi.org/10.1186/1471-2164-14-7.

[10] Gori, F., Tringe, S.G., Kartal, B., Machiori, E., Jetten, M.S.M. (2011) The metagenomic basis of anammox metabolism in *Candidatus* 'Brocadia fulgida'. Biochem. Soc. Trans. 39, 1799–1804, http://dx.doi.org/10.1042/BST20110707.

[11] Van de Graaf, A.A., de Bruijn, P., Robertson, L.A., Jetten, M.S.M., Kuenen, J.G. (1996) Autotrophic growth of anaerobic ammonium-oxidizing microorganisms in a fluidized bed reactor. Microbiology 142, 2187–2196, http://dx.doi.org/10.1099/13500872-142-8-2187.

[12] Güven, D., Dapena, A., Kartal, B., Schmid, M.C., Maas, B., van de Pas-Schoonen, K., Sozen, S., Mendez, R., Op den Camp, H.J.M., Jetten, M.S.M., Strous, M., Schmidt, I. (2005) Propionate oxidation by and methanol inhibition of anaerobic ammonium-oxidizing bacteria. Appl. Environ. Microbiol. 71, 1066–1071, http://dx.doi.org/10.1128/AEM.71.2.1066-1071.2005.

[13] Güven, D., van de Pas-Schoonen, K., Schmid, M.C., Strous, M., Jetten, M.S.M., Sözen, S., Orhon, D., Schmidt, I. (2004) Implementation of the anammox process for improved nitrogen removal. J. Environ. Sci. Health A 39, 1729–1738, http://dx.doi.org/10.1081/ESE-120037873.

[14] Hall, T. (1999) BioEdit: a user-friendly biological sequence alignment editor and analysis program for windows 95/98/NT. Nucleic Acids Symp. Ser. 41, 95–98.

[15] Hamersley, M.R., Woebken, D., Boehrer, B., Schultze, M., Lavik, G., Kuypers, M.M.M. (2009) Water column anammox and denitrification in a temperate permanently stratified lake (Lake Rassnitzer, Germany). Syst. Appl. Microbiol. 32, 571–582, http://dx.doi.org/10.1016/j.syapm.2009.07.009.

[16] Han, P., Klümper, U., Wong, A., Li, M., Lin, J.-G., Quan, Z., Denecke, M., Gu, J.-D. (2017) Assessment of molecular detection of anaerobic ammonium-oxidizing (anammox) bacteria in different environmental samples using PCR primers based on 16S rRNA and functional genes. Appl. Microbiol. Biotechnol. 101, 7689–7702, http://dx.doi.org/10.1007/s00253-017-8502-3.

[17] Harhangi, H.R., Le Roy, M., van Alen, T., Hu, B.-l., Groen, J., Kartal, B., Tringe, S.G., Quan, Z.-X., Jetten, M.S.M., Op den Camp, H.J.M. (2011) Hydrazine synthase, a unique phylomarker with which to study the presence and biodiversity of anammox bacteria. Appl. Environ. Microbiol. 78, 752–758, http://dx.doi.org/10.1128/AEM.07113-11.

[18] Hirsch, M.D., Long, Z.T., Song, B. (2011) Anammox bacterial diversity in various aquatic ecosystems based on the detection of hydrazine oxidase genes (*hzoA*/*hzoB*). Microb. Ecol. 61, 264–276, http://dx.doi.org/10.1007/s00248-010-9743-1.

[19] Hoekstra, M., de Weerd, F.A., Kleerebezem, R., van Loosdrecht, M.C.M. (2018) Deterioration of the anammox process at decreasing temperatures and long SRTs. Environ. Technol. 39, 658–668, http://dx.doi.org/10.1080/09593330.2017.1309078.

[20] Hou, L., Zheng, Y., Liu, M., Gong, J., Zhang, X., Yin, G., You, L. (2013) Anaerobic ammonium oxidation (anammox) bacterial diversity, abundance, and activity in marsh sediments of the Yangtze Estuary. J. Geophys. Res. Biogeosci. 118, 1237–1246, http://dx.doi.org/10.1002/jgrg.20108.

[21] Jenni, S., Vlaeminck, S.E., Morgenroth, E., Udert, K.M. (2014) Successful application of nitritation/anammox to wastewater with elevated organic carbon to ammonia ratios. Water Res. 49, 316–326, http://dx.doi.org/10.1016/j.watres.2013.10.073.

[22] Jetten, M., van Niftrik, L., Strous, M., Kartal, B., Keltjens, J., Op den Camp, H.J.M. (2009) Biochemistry and molecular biology of anammox bacteria. Crit. Rev. Biochem. Mol. Biol. 44, 65–84, http://dx.doi.org/10.1080/10409230902722783.

[23] Kartal, B., de Almeida, N.M., Maalcke, W.J., Op den Camp, H.J.M., Jetten, M.S.M., Keltjens, J.T. (2013) How to make a living from anaerobic ammonium oxidation. FEMS Microbiol. Rev. 37, 428–461, http://dx.doi.org/10.1111/1574-6976.12014.

[24] Kartal, B., Kuenen, J.G., van Loosdrecht, M.C.M. (2010) Sewage treatment with anammox. Science 328, 702–703, http://dx.doi.org/10.1126/science.1185941.

[25] Kartal, B., Maalcke, W.J., de Almeida, N.M., Cirpus, I., Gloerich, J., Geerts, W., Op den Camp, H.J.M., Harhangi, H.R., Janssen-Megens, E.M., Francoijs, K.-J., Stunnenberg, H.G., Keltjens, J.T., Jetten, M.S.M., Strous, M. (2011) Molecular mechanism of anaerobic ammonium oxidation. Nature 479, 127–130, http://dx.doi.org/10.1038/nature10453.

[26] Kartal, B., van Niftrik, L., Sliekers, O., Schmid, M.C., Schmidt, I., van de Pas-Schoonen, K., Cirpus, I., van der Star, W., van Loosdrecht, M., Abma, W., Kuenen, J.G., Mulder, J.-W., Jetten, M.S.M., den Camp, H.O., Strous, M., van de Vossenberg, J. (2004) Application, eco-physiology and biodiversity of anaerobic ammonium-oxidizing bacteria. Rev. Environ. Sci. Biotechnol. 3, 255–264, http://dx.doi.org/10.1007/s11157-004-7247-5.

[27] Kartal, B., van Niftrik, L., Rattray, J., van De Vossenberg, J.L.C.M., Schmid, M.C., Sinninghe Damsté, J., Jetten, M.S.M., Strous, M. (2008) *Candidatus* 'Brocadia fulgida': an autofluorescent anaerobic ammonium oxidizing bacterium. FEMS Microbiol. Ecol. 63, 46–55, http://dx.doi.org/10.1111/j.1574-6941.2007.00408.x.

[28] Kastner, V., Somitsch, W., Schnitzhofer, W. (2012) The anaerobic fermentation of food waste: a comparison of two bioreactor systems. J. Clean. Prod. 34, 82–90, http://dx.doi.org/10.1016/j.jclepro.2012.03.017.

[29] Kuenen, J.G. (2008) Anammox bacteria: from discovery to application. Nat. Rev. Microbiol. 6, 320–326, http://dx.doi.org/10.1038/nrmicro1857.

[30] Lamsam, A., Laohaprapanon, S., Annachhatre, A.P. (2008) Combined activated sludge with partial nitrification (AS/PN) and anammox processes for treatment of seafood processing wastewater. J. Environ. Sci. Health A 43, 1198–1208, http://dx.doi.org/10.1080/10934520802171766.

[31] Langone, M., Yan, J., Haaijer, S.C.M., Op den Camp, H.J.M., Jetten, M.S.M., Andreottola, G. (2014) Coexistence of nitrifying, anammox and denitrifying bacteria in a sequencing batch reactor. Front. Microbiol. 5, http://dx.doi.org/10.3389/fmicb.2014.00028.

[32] Li, M., Gu, J.-D. (2011) Advances in methods for detection of anaerobic ammonium oxidizing (anammox) bacteria. Appl. Microbiol. Biotechnol. 90, 1241–1252, http://dx.doi.org/10.1007/s00253-011-3230-6.

[33] Li, M., Hong, Y., Klotz, M.G., Gu, J.-D. (2010) A comparison of primer sets for detecting 16S rRNA and hydrazine oxidoreductase genes of anaerobic ammonium-oxidizing bacteria in marine sediments. Appl. Microbiol. Biotechnol. 86, 781–790, http://dx.doi.org/10.1007/s00253-009-2361-5.

[34] Liu, S.T., Horn, H., Müller, E. (2013) A systematic insight into a single-stage deammonification process operated in granular sludge reactor with high-loaded reject-water: characterization and quantification of microbiological community. J. Appl. Microbiol. 114, 339–351, http://dx.doi.org/10.1111/jam.12042.

[35] Lotti, T., Kleerebezem, R., Abelleira-Pereira, J.M., Abbas, B., van Loosdrecht, M.C.M. (2015) Faster through training: the anammox case. Water Res. 81, 261–268, http://dx.doi.org/10.1016/j.watres.2015.06.001.

[36] Neef, A., Amann, R., Schlesner, H., Schleifer, K.-H. (1998) Monitoring a widespread bacterial group: *in situ* detection of planctomycetes with 16S rRNA-targeted probes. Microbiology 144, 3257–3266, http://dx.doi.org/10.1099/00221287-144-12-3257.

[37] Op den Camp, H.J.M., Kartal, B., Guven, D., van Niftrik, L.A.M.P., Haaijer, S.C.M., van der Star, W.R.L., van de Pas-Schoonen, K.T., Cabezas, A., Ying, Z., Schmid, M.C., Kuypers, M.M.M., van de Vossenberg, J., Harhangi, H.R., Picioreanu, C., van Loosdrecht, M.C.M., Kuenen, J.G., Strous, M., Jetten, M.S.M. (2006) Global impact and application of the anaerobic ammonium-oxidizing (anammox) bacteria. Biochem. Soc. Trans. 34, 174–178, http://dx.doi.org/10.1042/BST0340174.

[38] Oshiki, M., Shimokawa, M., Fujii, N., Satoh, H., Okabe, S. (2011) Physiological characteristics of the anaerobic ammonium-oxidizing bacterium "*Candidatus* Brocadia sinica". Microbiology 157, 1706–1713, http://dx.doi.org/10.1099/mic.0.048595-0.

[39] Penton, C.R., Devol, A.H., Tiedje, J.M. (2006) Molecular evidence for the broad distribution of anaerobic ammonium-oxidizing bacteria in freshwater and marine sediments. Appl. Environ. Microbiol. 72, 6829–6832, http://dx.doi.org/10.1128/AEM.01254-06.

[40] Persson, F., Sultana, R., Suarez, M., Hermansson, M., Plaza, E., Wilén, B.-M. (2014) Structure and composition of biofilm communities in a moving bed biofilm reactor for nitritation–anammox at low temperatures. Bioresour. Technol. 154, 267–273, http://dx.doi.org/10.1016/j.biortech.2013.12.062.

[41] Rathsack, K., Böllmann, J., Martienssen, M. (2014) Comparative study of different methods for analyzing denitrifying bacteria in fresh water ecosystems. J. Water Resour. Prot. 6, 609–617, http://dx.doi.org/10.4236/jwarp.2014.66059.

[42] Schmid, M., Schmitz-Esser, S., Jetten, M., Wagner, M. (2001) 16S-23S rDNA intergenic spacer and 23S rDNA of anaerobic ammonium-oxidizing bacteria: implications for phylogeny and *in situ* detection. Environ. Microbiol. 3, 450–459, http://dx.doi.org/10.1046/j.1462-2920.2001.00211.x.

[43] Schmid, M., Twachtmann, U., Klein, M., Strous, M., Juretschko, S., Jetten, M., Metzger, J.W., Schleifer, K.-H., Wagner, M. (2000) Molecular evidence for genus level diversity of bacteria capable of catalyzing anaerobic ammonium oxidation. Syst. Appl. Microbiol. 23, 93–106, http://dx.doi.org/10.1016/S0723-2020(00)80050-8.

[44] Schmid, M., Walsh, K., Webb, R., Rijpstra, W.I., van de Pas-Schoonen, K., Verbruggen, M.J., Hill, T., Moffett, B., Fuerst, J., Schouten, S., Sinninghe Damsté, J.S., Harris, J., Shaw, P., Jetten, M., Strous, M. (2003) *Candidatus* "Scalindua brodae", sp. nov., *Candidatus* "Scalindua wagneri", sp. nov., two new species of anaerobic ammonium oxidizing bacteria. Syst. Appl. Microbiol. 26, 529–538, http://dx.doi.org/10.1078/072320203770865837.

[45] Schmid, M.C., Maas, B., Dapena, A., van de Pas-Schoonen, K., van de Vossenberg, J., Kartal, B., van Niftrik, L., Schmidt, I., Cirpus, I., Kuenen, J.G., Wagner, M., Sinninghe Damste, J.S., Kuypers, M., Revsbech, N.P., Mendez, R., Jetten, M.S.M., Strous, M. (2005) Biomarkers for *in situ* detection of anaerobic ammonium-oxidizing (anammox) bacteria. Appl. Environ. Microbiol. 71, 1677–1684, http://dx.doi.org/10.1128/AEM.71.4.1677-1684.2005.

[46] Schneckenburger, H., Reuter, B.W., Schoberth, S.M. (1984) Time-resolved fluorescence microscopy for measuring specific coenzymes in methanogenic bacteria. Anal. Chim. Acta 163, 249–255, http://dx.doi.org/10.1016/S0003-2670(00)81514-7.

[47] Strous, M., Heijnen, J.J., Kuenen, J.G., Jetten, M.S.M. (1998) The sequencing batch reactor as a powerful tool for the study of slowly growing anaerobic ammonium-oxidizing microorganisms. Appl. Microbiol. Biotechnol. 50, 589–596, http://dx.doi.org/10.1007/s002530051340.

[48] Tamura, K., Stecher, G., Peterson, D., Filipski, A., Kumar, S. (2013) MEGA6: molecular evolutionary genetics analysis version 6.0. Mol. Biol. Evol. 30, 2725–2729, http://dx.doi.org/10.1093/molbev/mst197.

[49] Van Hulle, S.W.H., Vandeweyer, H.J.P., Meesschaert, B.D., Vanrolleghem, P.A., Dejans, P., Dumoulin, A. (2010) Engineering aspects and practical application of autotrophic nitrogen removal from nitrogen rich streams. Chem. Eng. J. 162, 1–20, http://dx.doi.org/10.1016/j.cej.2010.05.037.

[50] Vanotti, M., Szogi, A., Rothrock, M., Novel anammox bacterium isolate. WO2011/094305A3, 2011.

[51] Winkler, M.K.H., Yang, J., Kleerebezem, R., Plaza, E., Trela, J., Hultman, B., van Loosdrecht, M.C.M. (2012) Nitrate reduction by organotrophic anammox bacteria in a nitritation/anammox granular sludge and a moving bed biofilm reactor. Bioresour. Technol. 114, 217–223, http://dx.doi.org/10.1016/j.biortech.2012.03.070.

[52] Woebken, D., Lam, P., Kuypers, M.M.M., Naqvi, S.W.A., Kartal, B., Strous, M., Jetten, M.S.M., Fuchs, B.M., Amann, R. (2008) A microdiversity study of anammox bacteria reveals a novel *Candidatus* Scalindua phylotype in marine oxygen minimum zones. Environ. Microbiol. 10, 3106–3119, http://dx.doi.org/10.1111/j.1462-2920.2008.01640.x.

[53] Zheng, Y., Jiang, X., Hou, L., Liu, M., Lin, X., Gao, J., Li, X., Yin, G., Yu, C., Wang, R. (2016) Shifts in the community structure and activity of anaerobic ammonium oxidation bacteria along an estuarine salinity gradient. J. Geophys. Res. Biogeosci. 121, 1632–1645, http://dx.doi.org/10.1002/2015JG003300.